10-14-2010

Seasonal Variability in Air-Sea Fluxes of CO_2 in a River-Influenced Coastal Margin

Steven E. Lohrenz
University of Southern Mississippi, slohrenz@umassd.edu

Wei-Jun Cai
University of Georgia, wcai@udel.edu

Fengwei Cai
University of Georgia

Xiaogang Chen
University of Southern Mississippi, Xiaogang.Chen@usm.edu

Merritt Tuel
University of Southern Mississippi

Follow this and additional works at: https://aquila.usm.edu/fac_pubs

Part of the Oceanography and Atmospheric Sciences and Meteorology Commons

Recommended Citation

Seasonal variability in air-sea fluxes of CO2 in a river-influenced coastal margin

5 authors, including:

Steven E Lohrenz
University of Massachusetts Dartmouth
162 PUBLICATIONS   **4,093** CITATIONS

Wei-Jun Cai
University of Delaware
164 PUBLICATIONS   **4,777** CITATIONS

Some of the authors of this publication are also working on these related projects:

Project   Collaborative Research - Ocean Acidification Category 1: Interactive Effects of Ocean Acidification, Temperature, and Nutrients on Coral Physiology and Calcification View project

Seasonal variability in air-sea fluxes of CO$_2$ in a river-influenced coastal margin

Steven E. Lohrenz,[1] Wei-Jun Cai,[2] Feizhou Chen,[2] Xiaogang Chen,[1] and Merritt Tuel[1]

[1] Recent studies in the northern Gulf of Mexico and elsewhere have demonstrated that enhanced biological production in large river plumes may contribute to a net surface influx of atmospheric CO$_2$. However, large rivers also deliver significant amounts of terrestrial carbon into continental margin waters; hence, the potential for large and variable signals in carbon flux exist in these regions. Here, we used a combination of satellite and ship-based observations to examine variability in surface pCO$_2$ and air-sea flux of carbon dioxide in relation to variations in river discharge and seasonal environmental conditions. Underway surface pCO$_2$ showed large seasonal differences based on observations acquired during cruises in August 2004, October 2005, and April 2006. Strong cross-shelf gradients in pCO$_2$ were observed during August 2004 and April 2006, influenced by river outflow. Uniformly high values observed during October 2005 likely reflected the disturbed nature of the system after two major storm events (hurricanes Katrina and Rita). Satellite-derived assessments of pCO$_2$ were used in conjunction with estimates of wind fields to produce regional maps of surface water pCO$_2$ and air-sea fluxes. The region was a net sink for atmospheric CO$_2$ in August 2004 (-0.96 to -1.2 mmol C m^{-2} d^{-1}) and net source during October 2005 and April 2006 (1.0 to 5.4 mmol C m^{-2} d^{-1}). Uncertainties in flux estimates, particularly for low salinity waters in April 2006, highlighted the need for more extensive in situ observations. Our results illustrate the utility of satellite approaches for providing regional assessments of coastal carbon budgets.

1. Introduction

[2] Flux of carbon dioxide between the atmosphere and the ocean is a critical term in global carbon cycle models. Coastal regions, despite their relatively small proportion of total surface area, can have a significant impact on global carbon budgets [*Borges*, 2005; *Borges et al.*, 2005; *Borges et al.*, 2006; *Cai et al.*, 2006]. Coastal margin ecosystems receive massive inputs of terrestrial organic and mineral matter and exhibit intense geochemical and biological processing of carbon and other elements. In addition, they exchange large amounts of matter and energy with the open ocean. The complex and variable nature of coastal margins poses significant challenges to efforts to characterize the carbon signals in these regions.

[3] Recent studies in the northern Gulf of Mexico [*Cai*, 2003; *Cai and Lohrenz*, 2010; *Lohrenz and Cai*, 2006] and in the Amazon River plume [*Kortzinger*, 2003; *Ternon et al.*, 2000] and Changjiang River plume/East China Sea

region [*Tsunogai et al.*, 1999; *Wang et al.*, 2000] have demonstrated that enhanced biological production in large river plumes associated with high−nutrient inputs may lead to very low surface water pCO$_2$ levels and a correspondingly high net surface influx of atmospheric CO$_2$. However, such major river systems also deliver large amounts of terrestrial organic and inorganic carbon into continental margin waters; hence, the potential for large and variable signals in carbon flux exists in river-dominated coastal regions [*Borges*, 2005; *Borges et al.*, 2005; *Chen et al.*, 2008]. The net effect of major processes on air-sea CO$_2$ exchange in river-dominated margins is not well known, and current estimates of their contribution to regional and global carbon budgets remain equivocal. This is particularly true for the northern Gulf of Mexico. Recent syntheses [*Cai et al.*, 2006; *Chavez et al.*, 2007; *Robbins et al.*, 2009] highlight the lack of information about the northern Gulf of Mexico and the need for additional data regarding carbon fluxes in the Gulf of Mexico.

[4] The Mississippi-Atchafalaya River ranks seventh in discharge among world rivers, drains approximately 40% of the conterminous United States (3.21 × 10^6 km^2; the third largest drainage basin among the world major rivers), and carries approximately 65% of all the suspended solids and dissolved solutes that enter the ocean from the United States

---

[1]Department of Marine Science, University of Southern Mississippi, Stennis Space Center, Mississippi, USA.
[2]Department of Marine Sciences, University of Georgia, Athens, Georgia, USA.
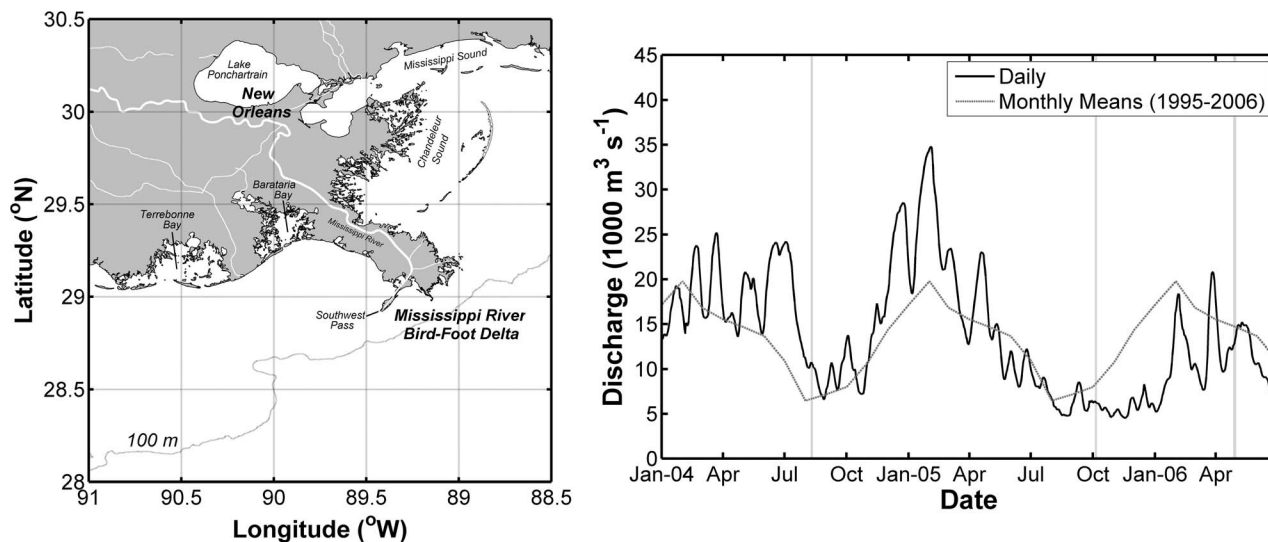
Figure 1. (left) A map of the study area illustrates major geographical features. The dashed line delineates the 100 m isobath, which roughly coincides with the shelf edge. (right) Cruises were conducted during different river discharge conditions. The solid line is Mississippi River discharge observations reported for Tarbert Landing, Miss. (Data courtesy of U.S. Army Corps of Engineers.) Vertical lines indicate cruise periods. River discharge is typically high in spring and early summer and declines into the fall, as illustrated by the dashed line which represents the monthly averaged flow for the period of 1995–2006.

[*Dagg et al.*, 2004; *Milliman and Meade*, 1983]. These materials are effectively injected onto the continental shelf as a point source in the northern Gulf of Mexico, and they substantially influence environmental conditions, including widespread hypoxia [*Rabalais et al.*, 2002] and the coastal carbon cycle [*Cai and Lohrenz*, 2010].

[5] A major objective of the U.S. Global Change Research Program, the U.S. Climate Change Science Program Strategic Plan, and the North American Carbon Program is the application of satellite ocean color to characterize the spatial variability of air-sea CO_2 flux in the oceans adjacent to the North American continent. Satellite-based regional approaches [*Jiang et al.*, 2008; *Lefevre et al.*, 2002; *Lohrenz and Cai*, 2006; *Olsen et al.*, 2004; *Ono et al.*, 2004] can be used to extend the spatial and temporal coverages for broadscale assessments of pCO_2 distributions and air-sea fluxes of CO_2. *Lohrenz and Cai* [2006] used such an approach to estimate regional distributions of surface pCO_2 and observed regions of low pCO_2 near the river plume based on a limited data set from June 2003. Calculations of regional air-sea flux showed a large net uptake of CO_2 in the region. Here, we expand on this earlier work using a combination of satellite and ship-based observations to examine variability in the surface water pCO_2 and air-sea flux of carbon dioxide in relation to variations in river discharge and seasonal conditions. This effort improves on that of *Lohrenz and Cai* [2006] in several aspects, including higher temporal and spatial data coverage and direct measurement of pCO_2 rather than indirect estimation from pH and dissolved inorganic carbon (DIC). Furthermore, we provide a more thorough examination of methods and uncertainties and associated implications for the utility of

satellite imagery for regional assessments of carbon system properties.

2. Methods

2.1. Cruise and Sampling Operations

[6] Cruises were conducted aboard the research vessel (R/V) *Pelican* during 9–12 August 2004, 4–7 October 2005, and 27 April–1 May 2006 in the outflow region of the Mississippi River (Figure 1, left). These cruises spanned a wide range of river discharge and seasonal conditions (Figure 1, right). Continuous underway measurements of surface salinity, temperature, and chlorophyll fluorescence were acquired with the ship's flow PC-based Multiple Instrument Data Acquisition System (MIDAS) using a Sea-Bird Electronics SBE 21 thermosalinograph, a Sea-Bird Electronics SBE 38 remote digital immersion thermometer, and a Turner Designs model 10 series fluorometer. Data from the ship's meteorological suite was also integrated, and sensors included an R.M. Young 05103 wind monitor, an R.M. Young model 61201 barometric pressure sensor, and an R.M. Young TS05327 temperature and relative humidity sensor.

[7] Underway determinations of sea surface pCO_2 were determined by directing flow from the ship's flow-through system through a "shower head equilibrator plus infrared detector (Li7000)" system to measure sea surface pCO_2, as described by *Wang and Cai* [2004].

[8] Absorption by colored dissolved organic matter (CDOM) (a_{CDOM}, m^{-1}) was determined by filtration of water samples through a 0.2 μm 47 mm diameter polycarbonate filter using a glass filtration apparatus. The filtrate was stored in a dark amber glass bottle with a Teflon-lined
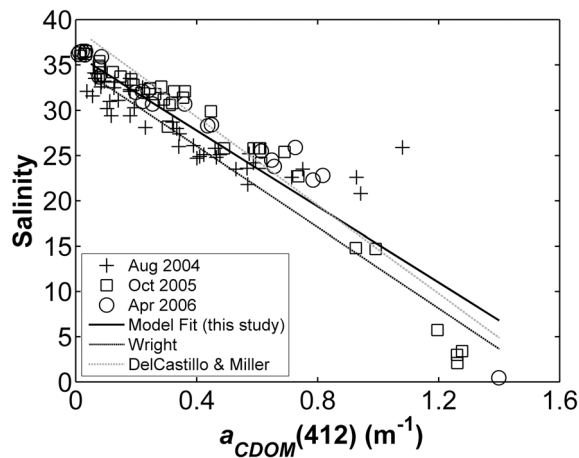
Figure 2. A consistent relationship was observed between chromophoric dissolved absorption at 412 nm, $a_{CDOM}(412)$, and salinity for the Mississippi River outflow region for all three cruise periods. The solid line represents a linear regression fit to the data as given by the following relationship: salinity = $36.2 - 21.0 a_{CDOM}(412)$ ($r^2 = 0.863$, $N = 99$). For comparison, relationships are shown for *Wright* [2005] and *Del Castillo and Miller* [2008].

cap, and it was refrigerated until analysis. Within two weeks, a_{CDOM} was determined using a Cary 300 bio-UV-visible spectrophotometer in the lab, using 10 cm quartz cells with Milli-Q® water as a blank. We observed a strong correlation between a_{CDOM} and salinity that was consistent for all three cruises (Figure 2). A linear regression fit to the data produced the following relationship:

$$\text{salinity} = 36.2 - 21.0 a_{CDOM}(412)\left(r^2 = 0.863, N = 99\right). \quad (1)$$

This relationship was similar to those previously reported by *Wright* [2005] and *Del Castillo and Miller* [2008] for the Mississippi River plume region (Figure 2).

2.2. Estimation of Chlorophyll Concentrations from Pigment Absorption and Underway Fluorescence

[9] To estimate chlorophyll concentrations from underway fluorescence, empirical relationships between fluorescence and pigment absorption at 676 nm (as a proxy for chlorophyll concentration) were determined. Chlorophyll concentrations were then estimated from absorption at 676 nm by dividing by a factor of 0.021 m^{-2} mg chlorophyll a^{-1} [*Lohrenz et al.*, 2003]. Pigment absorption was determined using the quantitative filter pad technique, as described by *Lohrenz et al.* [2003]. Briefly, samples were filtered onto a Whatman 25 mm GF/F filter and stored in liquid nitrogen until analysis. The transmittance of filters was determined with a Perkin Elmer Lambda 18 spectrophotometer equipped with a Labsphere 150 mm integrating sphere. Filters moistened with seawater filtrate were placed on a quartz slide at the entrance of the sphere and scanned from 350 to 800 nm at a scan speed of 120 nm min^{-1}. Slit width was 2 nm. Following the measurement of transmittance, pigments were extracted from the filter pad using a 15 min. extraction in hot methanol. The extracted filters were rinsed with Milli-Q water to remove residual methanol and phycobiliproteins,

and the measurements of transmittance were repeated to obtain the absorption spectrum of the particulate detrital material. Particulate absorption a_p (m^{-1}) was calculated as follows:

$$a_p = \frac{A_f}{\beta d_g \left(1 - A_f\right)}, \quad (2)$$

where A_f is the absorptance of the filter, β is the path length amplification factor (taken here as 2.7 after *Lohrenz et al.* [2003]), and d_g is the geometric path length (m) equivalent to the product of volume filtered and the clearance area of the filter. Absorptance A_f was determined from measurements of the transmittance of sample and blank filters, T_s and T_b, respectively, as given by the expression,

$$A_f = 1 - \frac{T_s}{T_b}. \quad (3)$$

The above-mentioned equations were applied to filters and methanol-extracted filters to obtain total particulate and detrital absorption, respectively. Pigment absorption a_{ph} (m^{-1}) was determined by subtraction of detrital absorption from the total particulate absorption.

[10] Regression analyses for each cruise yielded the following empirical relationships between pigment absorption at 676 nm, $a_{ph}(676)$, and underway chlorophyll fluorescence, F_{chl}, as follows:

$$\text{August 2004}: a_{ph}(676) = 0.00198 F_{chl}$$
$$+ 0.00991 \left(r^2 = 0.963; N = 31\right), \quad (4)$$

$$\text{October 2005}: a_{ph}(676) = 0.00206 F_{chl}$$
$$+ 0.00252 \left(r^2 = 0.968; N = 14\right), \quad (5)$$

$$\text{April 2006}: a_{ph}(676) = 0.00480 F_{chl}$$
$$+ 0.0216 \left(r^2 = 0.965; N = 18\right), \quad (6)$$

F_{chl} in this case corresponded to the chlorophyll fluorescence determined with the ship's flow-through system while on station.

2.3. Satellite-Ocean Color Extrapolation of pCO$_2$

[11] A satellite ocean-color algorithm was used for assessment of areal distributions of sea surface pCO$_2$ from Moderate Resolution Imaging Spectroradiometer (MODIS) imagery based on empirical relationships of in situ measurements of surface water pCO$_2$ and environmental variables, as previously described by *Lohrenz and Cai* [2006]. Briefly, the method involves application of principal component analysis (PCA) to the ship-based underway measurements of sea surface temperature (SST), salinity (SSS), and fluorescence-derived chlorophyll data. PCA is a statistical technique that reduces a possibly correlated set of variables to a subset of independent or orthogonal variables referred to as components. *Murata* [2006] used PCA to examine statistical relationships between pCO$_2$ and other variables in the eastern Bering Sea. Our approach differed from *Murata* [2006] in that we included only environmental

variables (SST, SSS, and chlorophyll) in the PCA with the goal of deriving an independent set of component variables that could then be used as predictors of $p\text{CO}_2$. Data were partitioned according to salinity ranges of <20, 20–28, and >28. The partitioned data were then subsampled by using every other value, such that half the data were used as a "training" data set to derive the principal components. The resulting principal components were then regressed against the corresponding $p\text{CO}_2$ values to produce an empirical algorithm for the estimation of $p\text{CO}_2$. The algorithm was evaluated using the remaining "test" data by determining the relationship between measured and estimated $p\text{CO}_2$. A portion of the high-salinity data acquired near the river mouth were excluded from the analysis of the April 2006 data set because these observations deviated from the overall regression relationship developed for the bulk of the other data (not shown). These data were in the salinity range of 28–32. We attributed the deviation to the highly dynamic and spatially heterogeneous nature of the river plume in this region, which resulted in temporal offsets between the $p\text{CO}_2$ measurements and the sea surface temperature (T) and salinity (S) measurements due to slight differences in sensor response times.

[12] An analogous set of environmental products was derived from ocean color satellite imagery acquired from the MODIS aboard the Aqua satellite. Image data were acquired from the NASA Goddard Space Flight Center Ocean Color Web [*Feldman and McClain*, 2007]. Level 0 files were processed to the 250 m resolution level 2 products and mapped using the SeaWiFS Data Analysis System (Sea-DAS) data analysis system version 5.2 [*Baith et al.*, 2001]. Products included chlorophyll a (chlor_a), detrital and dissolved absorption at 412 nm (adg_412_gsm01), and sea surface temperature (SST). The chlor_a product was determined using the OC3M chlorophyll a algorithm, and the adg_412_gsm01 product was derived using the Garver-Siegel-Maritorena, version 1, semianalytical algorithm [*Maritorena et al.*, 2002]. Surface water salinities were derived from the adg_412_gsm01 product using the relationship given in equation 1 (Figure 2). The derived satellite products were used, along with the derived empirical algorithm, to estimate $p\text{CO}_2$ for a given image. The adg_412_gsm01 product was assumed to be representative of a_{CDOM} at 412 nm, as measured on discrete samples as described previously. We assumed that the majority of the adg_412_gsm01 product absorption was due to the dissolved fraction, which is reasonable in view of prior findings of strong relationships between in situ measurements of a_{CDOM} and analogous satellite-derived products [*D'Sa et al.*, 2006; *Del Castillo and Miller*, 2008].

[13] Because of cloud contamination, it was not always possible to obtain contemporaneous imagery for the cruise periods. For August 2004, an acceptably clear image was obtained for 15 August 2004, which was three days after the cruise period (9–12 August 2004). Only in situ data from the latter part of the cruise (11–12 August 2004) were used in determining matchups to reduce the temporal offset between satellite and in situ observations. For October 2005, a five-day image composite was produced from a series of images acquired on 2–6 October 2005, significantly overlapping the cruise period of 4–7 October 2005. For April 2006, a two-day image composite was generated from images acquired

on 23–24 April 2006, which preceded the cruise period of 27 April–1 May 2006. In situ data for determining satellite matchups were restricted to data from the beginning of the cruise (27–30 April 2006) again to reduce the temporal offset between satellite and in situ observations. These dates were chosen because of the passage of a frontal system around 30 April 2006, which substantially altered hydrographic conditions.

2.4. Air-Sea Flux of Carbon Dioxide

[14] Satellite-derived regional assessments of sea surface $p\text{CO}_2$ were used in conjunction with estimates of wind fields to produce regional-scale estimates of air-sea fluxes. Following the convention of *Jiang et al.* [2008], the air-sea flux of carbon dioxide F_{CO_2} can be estimated as

$$F_{CO_2} = k\,K_0\,(pCO_{2water} - pCO_{2air}), \qquad (7)$$

where k (cm h^{-1}) is the gas transfer velocity (piston velocity) of CO₂, K_0 (mol L^{-1} atm^{-1}) is the solubility coefficient of CO₂ at the in situ temperature and salinity, and pCO_{2water} and pCO_{2air} (μatm) are the water-saturated partial pressures of CO₂ in the water and the air, respectively. Positive values of F_{CO_2} indicate a transfer of CO₂ from the water to the atmosphere. Ship-based atmospheric measurements of CO₂ from the cruises were compromised due to contamination by the ship's exhaust. Instead, for flux calculations, an air $p\text{CO}_2$ value of 380 μatm was used based on global average atmospheric $p\text{CO}_2$ values obtained from the NOAA Earth System Research Laboratory [*Tans*, 2009]. For comparison, averaged values for atmospheric $p\text{CO}_2$ measured in the nearby South Atlantic Bight during April, August, and October 2005 were 382, 378, and 380 μatm, respectively [*Jiang et al.*, 2008].

[15] The gas transfer velocities were adjusted for variability over a given monthly period by determining non-linearity coefficients, as described by *Jiang et al.* [2008]. Various sets of the gas transfer velocity k vs. wind speed relationships (see section 3) were used to bracket the gas flux. Wind speeds for August 2004 and April 2006 were estimated from data provided by the NOAA National Data Buoy Center C-Man Station BURL1, located at 28.90°N 89.43°W near Southwest Pass. For October 2005, data were obtained from buoy station 42040, 118 km south of Dauphin Island, Alabama, at 29.205°N 88.205°W. For flux calculations, satellite-derived estimates of surface water $p\text{CO}_2$ in excess of 1000 μatm were discarded, as such values were observed only in the Mississippi River itself, and they were considered to be unreliable for other areas of the image where in situ observations were lacking.

3. Results

3.1. River Discharge Patterns

[16] River discharge data were acquired from the U.S. Army Corps of Engineers for the Tarbert Landing discharge site (gage 01100) located at approximately river mile 306.3. This site was chosen, as it is located below the Old River Control Structure, which diverts water to the Atchafalaya River such that, of the flow coming from the entire Mississippi-Atchafalaya basin, the distribution between the Mississippi and Atchafalaya rivers is 70 and 30%, respec-
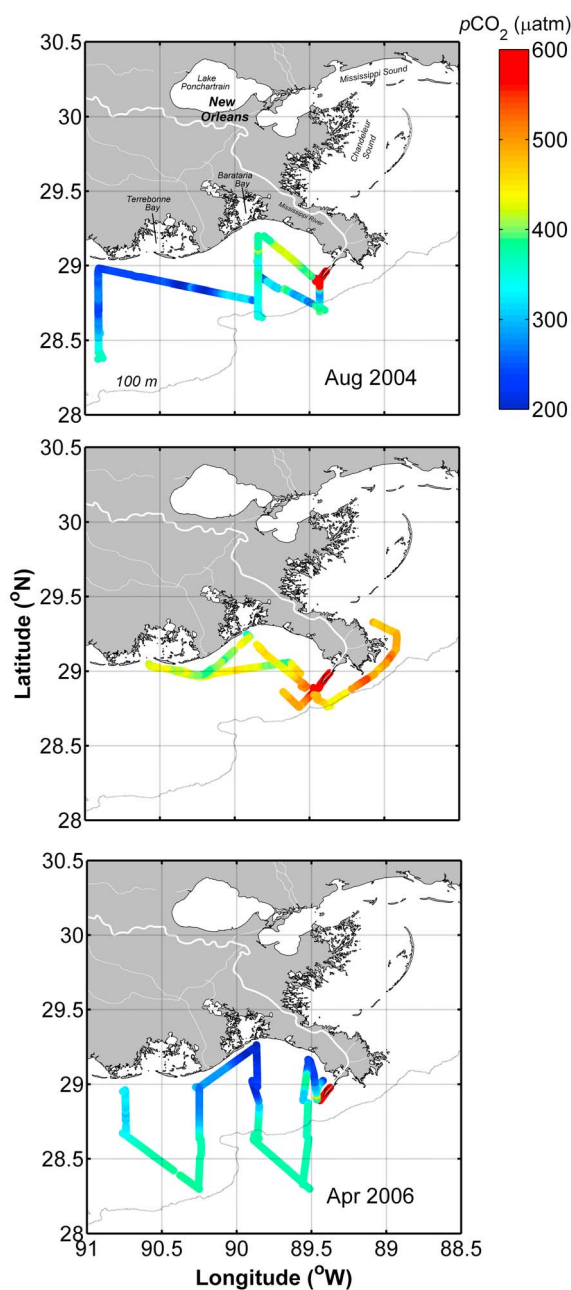
Figure 3. Shipboard underway observations reveal relatively low values of surface pCO_2 in the vicinity of the river outflow during August 2004 and April 2006. During October 2005, values were generally higher than observed during the other cruises. For all cruises, highest values of pCO_2 were observed in river waters near Southwest Pass.

tively [*Goolsby et al.*, 1999]. As there are no other major locks or dams on the river below Tarbert Landing, the discharge at this site is considered to be representative of that exiting through the Belize (or Bird's Foot) delta (Figure 1, left).

[17] The three cruises encompassed a variety of river discharge and seasonal conditions (Figure 1, right). The August 2004 cruise came at a period of relatively low flow that had been preceded by a period of relatively high river

discharge. The October 2005 cruise coincided with a period of low river flow that followed Hurricane Katrina, which made landfall on 29 August 2005 in the vicinity of southeast Louisiana and western Mississippi, and Hurricane Rita, which made landfall on 23 September 2005 near the Texas-Louisiana border. These events dramatically impacted the region and were accompanied by substantial vertical mixing of coastal waters and coastal flooding. The April 2006 cruise occurred during a period of increasing river discharge, although discharge during the 2006 season was generally below average (Figure 1, right). Thus, discharge during these three cruises ranged from low (August and October) to intermediate (April) levels.

3.2. Distributions of Surface pCO_2 From Underway Shipboard Surveys

[18] Surface maps of pCO_2 revealed strong spatial gradients in pCO_2 values (Figure 3). The highest values were associated with regions influenced by river outflow. During the August 2004 cruise, there was a strong alongshelf gradient, with the lowest surface pCO_2 values located in the western portion of the sampling region off Terrebonne Bay. Values during October 2005 were uniformly higher than observed in other cruises. Areal coverage during this cruise was limited because of weather conditions. In April 2006, there was a strong cross-shelf gradient in pCO_2, with the lowest values nearshore and the values approaching atmospheric levels (~ 380 μatm) offshore.

3.3. Empirical Algorithm to Estimate pCO_2 From Environmental Variables

[19] Principal component analysis of the training data for ship-based underway sea surface T, S, and fluorescence-derived chlorophyll (Chl) revealed that the vast majority of the variance in the original variables could be explained by the first (PC1) and second (PC2) components (Table 1). Distinct differences in relationships among variables to the derived orthogonal components were evident in biplots of the loadings (Figure 4). In general, S and Chl behaved independently (were orthogonal to one another), and were generally strongly correlated with either the first (PC1) or second (PC2) components. Derived principal components were weakly correlated with T, an indication that T contributed in a minor way to the overall environmental variation within a given salinity range and cruise period.

[20] The regression of the derived principal components for the training data against the corresponding values of pCO_2 yielded component coefficients for the various cruises and salinity ranges (Table 2). Using the principal component scores for the individual variables derived from the training data, the representation of the test data in principal component space was determined and used in conjunction with the component coefficients in Table 2 to estimate pCO_2 for the test data set (Figure 5). Results of the correlation analysis of the estimated versus observed pCO_2 for the test data, including r^2 and probabilities, are given in Table 2. In all cases, the correlations were statistically significant ($p <$ 0.001) and, in most cases, r^2 values were greater than 0.7. Exceptions were in the case of the midsalinity data in August 2004 and the high salinity data in October 2005. For these data subsets, a combination of scatter and a limited dynamic range resulted in lower r^2 values.

Table 1. Percentage of Variance in Training Input Variables Explained by Principal Components

Salinity Range	Date	PC1	PC2	Total
<20	Aug 2004	99.9	0.10	100
	Oct 2005	91.6	8.4	100
	Apr 2006	96.3	3.6	99.9
20–28	Aug 2004	78.9	21.1	100
	Oct 2005	74.1	24.4	98.5
	Apr 2006	67.0	33.0	100
>28	Aug 2004	74.4	24.6	99.0
	Oct 2005	80.0	18.1	98.1
	Apr 2006	92.1	7.9	100

3.4. Satellite-Derived pCO_2 Distributions

[21] The strong influence of freshwater inputs was evident in an examination of satellite-derived distributions of pCO_2 (Figure 6). Regions of reduced-surface pCO_2 were evident in the vicinity of the river and the inner shelf regions during August 2004 and April 2006. In contrast, in October 2005, there was no apparent reduction associated with river outflow. Match ups between satellite and in situ pCO_2, binned by salinity range, showed general consistency in observed versus satellite-derived values (Figure 7). However, satellite-derived estimates were low in comparison to observed values of pCO_2 at low salinities during August 2004 and April 2006, while showing better agreement at midsalinities to high salinities (Figure 7). For other salinity ranges, satellite-derived values tended to overestimate pCO_2, including the salinities of 24–26 in August 2004 and 10–20 in April 2006.

3.5. Air-Sea Flux of CO_2

[22] Estimates were made using various flux parameterizations for different subregions representative of the outflow plume of the Mississippi River and for shelf water, as well as for the entire image (Figure 8 and Table 3). Air-sea flux of CO_2 was estimated from equation (7) using three sets of parameters, including those given by *Wanninkhof* [1992], *Nightingale et al.* [2000], and *Ho et al.* [2006]. There was an estimated net uptake of CO_2 in August 2004 for plume waters, while shelf waters were a weak source of CO_2 (Table 3). A net uptake of CO_2 was also estimated for the entire image region during August 2004. Similarly, in April 2006, mean fluxes for both plume and shelf waters
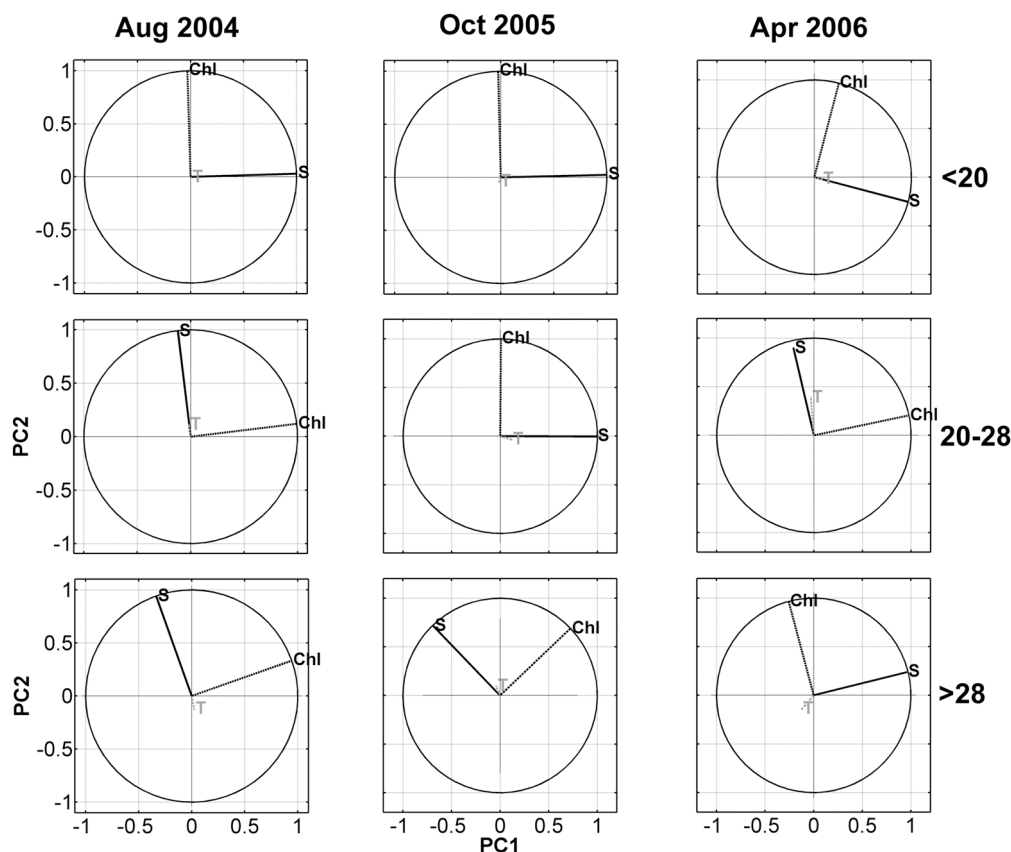

Figure 4. The principal component analysis (PCA) biplots for each salinity interval and cruise period illustrate relationships of the original variables (salinity, chlorophyll, and temperature) in the training data set to the derived component variables. Each vector represents the relationship of an original variable (i.e., *T*, *S*, or *Chl*) to the derived orthogonal components (PC1 and PC2). The length of the vector corresponds to the amount of variability in the original variable accounted for by the principal component variables. In cases where a vector aligns with one of the component axes, this indicates a strong correlation with that derived principal component variable. Percentage variation in the original data accounted for by each component is given in Table 1.

Table 2. Regression Results for Relationship Between Principal Components and Pco$_2$ for the Test Data

Salinity Range	Date	PC1 Coefficient	PC2 Coefficient	Intercept	r^2	p	N
<20	Aug. 2004	−71.7	138	1310	0.954	<0.001	46
	Oct. 2005	−56.6	12.1	1097	0.976	<0.001	64
	Apr. 2006	−57.2	−33.6	1002	0.952	<0.001	31
20–28	Aug. 2004	−12.2	3.30	308	0.245	<0.001	979
	Oct. 2005	−14.7	−45.0	483	0.860	<0.001	71
	Apr. 2006	−4.27	−31.4	267	0.756	<0.001	184
>28	Aug. 2004	−12.3	4.55	341	0.708	<0.001	266
	Oct. 2005	4.13	−15.8	450	0.165	<0.001	598
	Apr. 2006	16.6	−7.86	340	0.932	<0.001	669

reflected a net sink for atmospheric CO$_2$, while the entire image region was a weak source of CO$_2$ to the atmosphere (Table 3). Fluxes for October 2005 were estimated to be a net source of CO$_2$ for all regions, as well as for the entire image. Results were generally consistent among the different gas transfer parameterizations (Table 3).

4. Discussion

4.1. The pCO$_2$ Distributions

[23] Our findings suggest that the late spring and early summer in the river-influenced region of the northern Gulf of Mexico are periods of lower surface pCO$_2$ corresponding to a strong biological pump and relatively high autotrophic fixation of inorganic carbon. Other key environmental drivers appear to be seasonal variations in temperature and levels of freshwater discharge. The August 2004 cruise coincided with a period of relatively low river discharge (Figure 2), but it was preceded by a period of above-average river discharge. Nutrient-rich freshwater inputs have been shown to enhance primary production in this region [*Dagg and Breed*, 2003; *Dagg et al.*, 2004; *Lohrenz et al.*, 1990; *Lohrenz et al.*, 2008b; *Lohrenz et al.*, 1997; *Riley*, 1937] and are believed to contribute to a drawdown of carbon dioxide in the region [*Cai*, 2003; *Lohrenz and Cai*, 2006]. Areas of reduced pCO$_2$ were evident in August 2004, as well as in April 2006 (Figure 6). The April 2006 period coincided with relatively high river flow (Figure 2). The April 2006 imagery also shows regions of relatively high surface pCO$_2$ adjacent to the river delta and in inner shelf waters. The Mississippi River waters are characterized by high alkalinity and associated high dissolved inorganic carbon concentrations [*Cai*, 2003; *Cai and Lohrenz*, 2010; *Cai et al.*, 2008; *Lohrenz and Cai*, 2006], which could account for the initially high values of surface pCO$_2$ adjacent to the outflow region. The extent of these regions of high pCO$_2$ is unclear, particularly for the inner shelf regions where in situ data were lacking. Satellite-derived estimates of these features should be treated with a high degree of uncertainty. To a large extent, the satellite estimates of high inner shelf pCO$_2$ values stemmed from corresponding estimates of low salinity from the relationship to CDOM given in Figure 2. While this relationship is robust for large areas of the river plume and shelf [*Del Castillo and Miller*, 2008; *Wright*, 2005], its applicability to inner shelf regions is less certain due to the presence of multiple sources of CDOM in inner shelf regions that are not necessarily directly linked to river inputs. Therefore, an assessment of the validity of these estimates requires more extensive observations particularly in inner shelf waters.

[24] In contrast to the August 2004 and April 2006 periods, distributions of pCO$_2$ during October 2005 were generally high (Figure 6), and no apparent drawdown was evident in the vicinity of the river outflow. River discharge was quite low in October 2005 (Figure 1), and this cruise followed hurricanes Katrina and Rita [*Lohrenz et al.*, 2008a], which devastated the northern Gulf of Mexico coast and caused extensive coastal flooding. It is possible that the introduction of terrestrially derived organic matter associated with storm surge inundation, as well as destratification and the resuspension of bottom sediments, may have contributed to high levels of remineralization and associated high levels of pCO$_2$.

4.2. Comparison of Algorithms From Different Cruises

[25] A key question is the degree to which satellite imagery can be used to provide regional assessments of dissolved inorganic carbon system properties over extended time scales. The answer depends on the extent to which algorithms can be generalized beyond a single set of in situ observations. We examined this question by comparing principal component loadings and regression coefficients among the different periods (Table 2). As is discussed in subsequent paragraphs, results of the multiple regression analysis of component variables versus pCO$_2$ revealed both similarities and differences among the different cruise periods.

[26] In all cases for the low-salinity data sets, pCO$_2$ was negatively correlated with PC1 (Table 2), and PC1 was strongly correlated with salinity (Figure 4). This was consistent with an observed decrease in surface pCO$_2$ in relationship to increasing salinity, as seen in underway survey data when S < 20 (X. Guo, unpublished data, 2009). Such a relationship is expected in light of the fact that the river has relatively high levels of alkalinity and dissolved inorganic carbon [*Cai*, 2003], which would be expected to decrease as a result of mixing with ocean water. The relationship of pCO$_2$ to chlorophyll was more variable for the low salinity, which was evidenced by the fact that chlorophyll was generally strongly correlated with the second principal component (PC2, Figure 4), and the regression coefficients for this component were much more variable (Table 2).

[27] For the midsalinity data sets (20 ≤ S < 28), chlorophyll showed a strong relationship to PC1 in August 2004 and April 2006 (Figure 4) and to PC2 in October 2005 but, in all cases, the corresponding regression coefficients were negative (Table 2), indicating a negative relationship between chlorophyll and pCO$_2$ for this salinity range. The midsalinity region corresponds to what is referred to as the "optimal growth zone" [*DeMaster et al.*, 1996; *Lohrenz et al.*, 1999], where opposing gradients in nutrients and
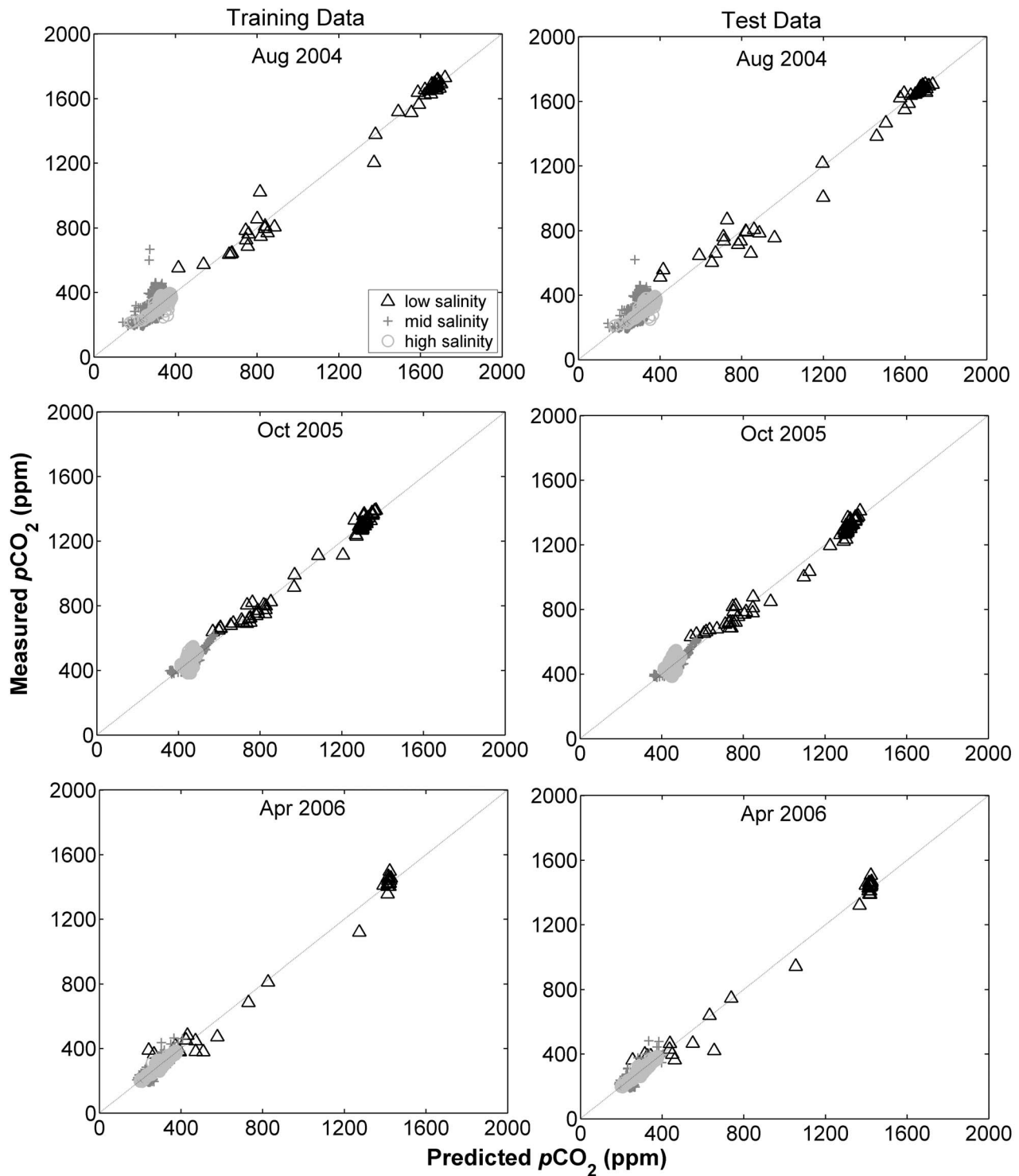
Figure 5. Estimates of pCO_2 from PCA-derived empirical algorithms showed strong correlations between measured and predicted pCO_2. Values of r^2 for test data were 0.939 ($N = 1291$), 0.974 ($N = 736$), and 0.983 ($N = 884$) for August 2004, October 2005, and April 2006, respectively.

light availability result in favorable conditions for primary production and phytoplankton growth. Increasing primary production and growth could produce a drawdown in surface pCO_2 and would explain the negative relationship to chlorophyll. Salinity was correlated with PC2 in August 2004

and April 2006 and with PC1 in October 2005, with both positive (August 2004) and negative (October 2005 and April 2006) regression coefficients (Table 2) that varied in magnitude. Thus, there was not a consistent relationship between salinity and pCO_2 for the midsalinity data.
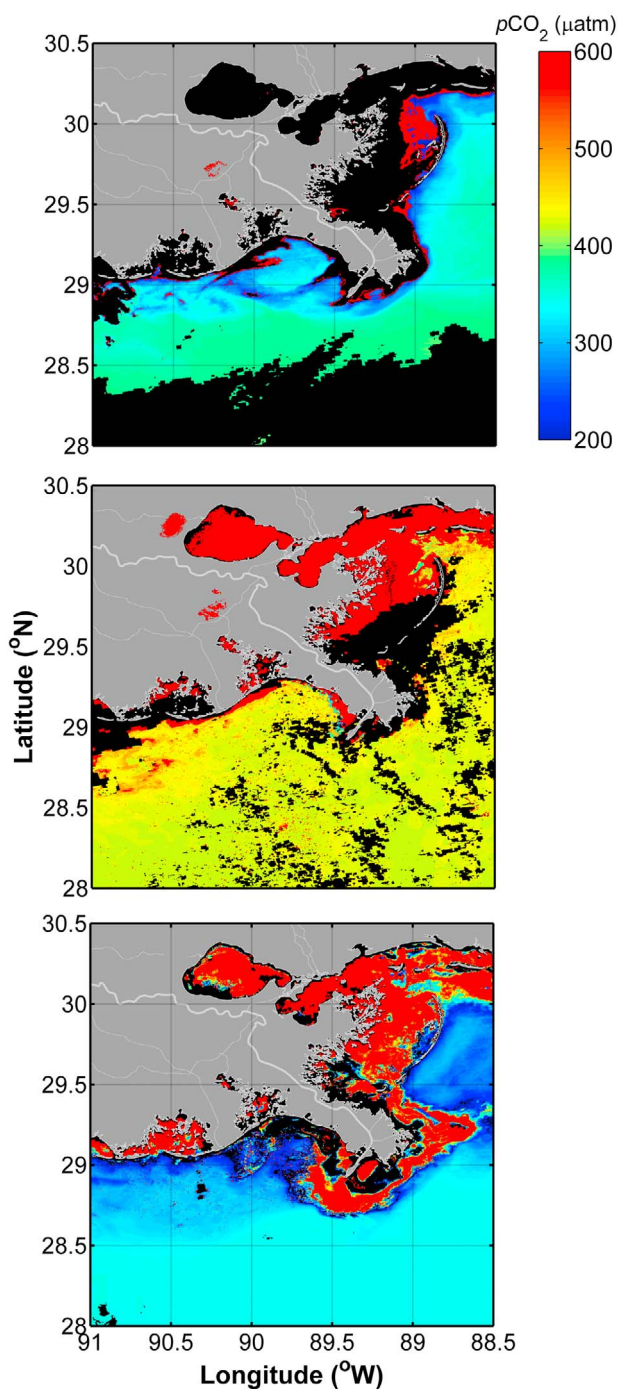
Figure 6. Satellite-derived estimates of surface water pCO_2 showed large seasonal differences, with lower values in inner shelf waters observed during August 2004, strong spatial gradients in nearshore pCO_2 in April 2006, and uniformly high values during October 2005. Black pixels correspond to areas where satellite observations were masked due to clouds or high turbidity.

[28] Finally, for the August 2004 high-salinity data (S > 28), salinity was most strongly correlated with PC2 and chlorophyll was most strongly correlated with PC1 (Figure 4), and regression coefficients were negative for PC1 and positive for PC2 (Table 2), indicating a negative rela-

tionship of pCO_2 with chlorophyll and positive relationship of pCO_2 with salinity. This is consistent with increasing values of surface pCO_2 with increasing salinities and decreasing chlorophyll concentrations offshore. Similarly, for April 2006, salinity was most strongly correlated with PC1 and chlorophyll was most strongly correlated with PC2 (Figure 4), and regression coefficients were positive for PC1
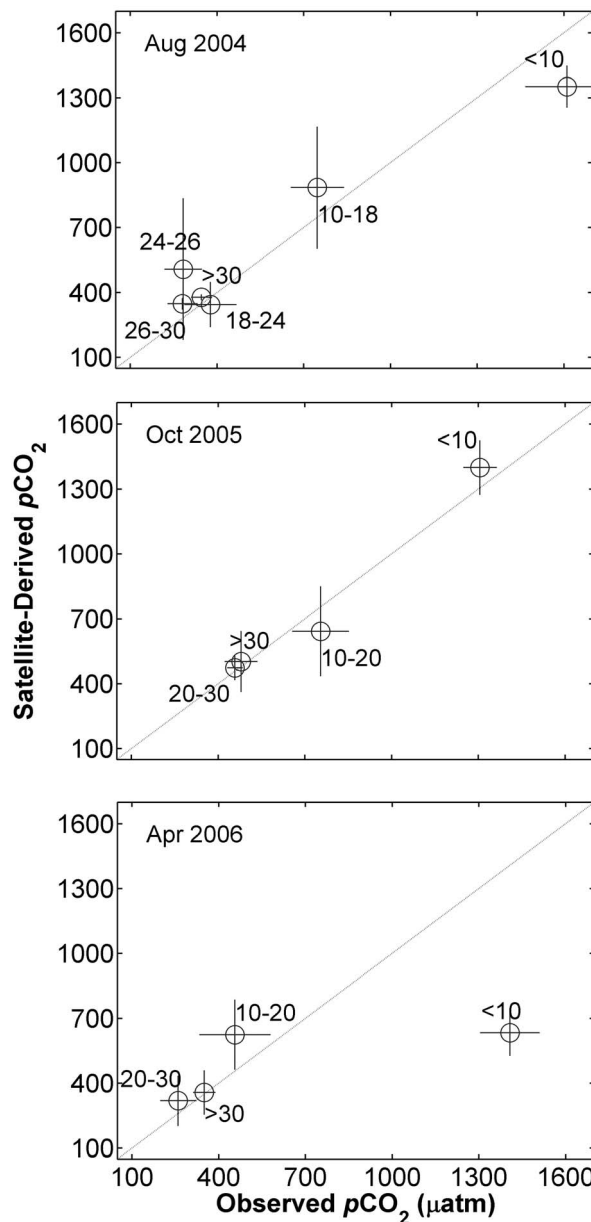

Figure 7. Match ups between satellite-derived and in situ pCO_2 binned by salinity range showed generally good agreement, with the exception of the <10 salinity data in August 2004 and April 2006, the 24–26 salinity range data during August 2004, and the 10–20 salinity range data during April 2006. Greater variability in the plume region and temporal offsets between the times for acquiring in situ and satellite data contributed to the differences between match ups at lower salinities.
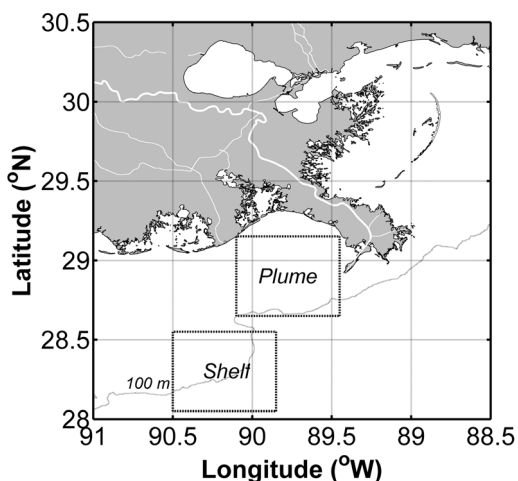
Figure 8. Geographic boundaries are shown for plume and shelf regions used to estimate the air-sea flux of CO$_2$ in Table 3.

and negative for PC2 (Table 2). This again reflects a negative relationship of pCO$_2$ with chlorophyll and a positive relationship of pCO$_2$ with salinity. For the October 2005 salinity data, the interpretation was less clear, as partial correlations of PC1 and PC2 with both chlorophyll and salinity were evident (Figure 4) with negative and positive regression coefficients (Table 2). Salinity was negatively correlated with PC1 and positively correlated with PC2, and regression coefficients were positive and negative for PC1 and PC2, respectively, which was consistent with a negative relationship between salinity and pCO$_2$. However, the October 2005 regression explained a relatively small amount of the variation in pCO$_2$, largely due to the fact that the data spanned a relatively small range of values. As such, the predictive skill of this relationship was limited.

[29] To summarize, some consistent trends were evident in the relationships between pCO$_2$ and environmental variables. Specifically, a consistent negative relationship between salinity and pCO$_2$ was observed for the low-salinity data and between chlorophyll and pCO$_2$ for the midsalinity data. For the high-salinity data, relationships of pCO$_2$ with chlorophyll were negative and relationships of pCO$_2$ with salinity were positive for the August 2004 and April 2006 data.

4.3. Uncertainties in Satellite-Derived pCO$_2$ Estimates

[30] The regression results highlight the complex relationship between surface pCO$_2$ and environmental variables and suggest that a "universal" algorithm for estimating pCO$_2$ from satellite-derived variables may be elusive. Nonetheless, the relatively high predictive skill of the regression relationships (Figure 5) and the general consistency between satellite match ups and in situ observations of pCO$_2$ (Figure 7) support the feasibility of extrapolating pCO$_2$ distributions from satellite observations. We acknowledge that, in some cases, the satellite observations diverged from the in situ observations. This was particularly evident in the case of the <10 salinity data during August 2004 and April 2006, for the 24–26 salinity range in August 2004, and for the 10–20 salinity range in April 2006 (Figure 7). Match-up data for these

salinity ranges generally corresponded to the highly dynamic plume region. Discrepancies between satellite-derived estimates and in situ observations for this region could have been due to a variety of factors. The distribution of the plume core can change rapidly in response to wind and coastal currents. Furthermore, conditions within plume waters can vary dramatically due to changing hydrodynamics and this may, in turn, influence biological activity and its impact on pCO$_2$ levels. In addition, the fact that composite imagery was used during October 2005 and April 2006 would tend to smooth out fine-scale features. Therefore, it is not surprising that there were differences between satellite-derived estimates and in situ observations for these periods.

4.4. Sensitivity of Air-Sea Flux Estimates to pCO$_2$ Uncertainties

[31] We considered the sensitivity of air-sea flux estimates to uncertainties in satellite-derived pCO$_2$ concentrations, basing estimates of uncertainty on differences between mean values of the satellite-derived pCO$_2$ concentrations and corresponding in situ pCO$_2$ values for specified salinity ranges (Figure 7). In the case of the August 2004 <10 salinity data, the mean value for satellite-derived pCO$_2$ was 1250 μatm, compared to a mean in situ value of 1610 μatm. Thus, the mean satellite-derived pCO$_2$ in the <10 salinity range was lower than the in situ mean by about 22%. In the case of April 2006, the mean value for satellite-derived pCO$_2$ in the <10 salinity range was 634 μatm, compared to a mean in situ value of 1410 μatm, a difference of about 55%. For both August 2004 and April 2006, the low-salinity in situ data were primarily acquired either in the Mississippi River channel or near the mouth (Figure 3). Assuming that the in situ match-up data were representative of other low-salinity pixels in the images where in situ data were lacking; then the sensitivity of air-sea flux estimates to potential biases in pCO$_2$ values can be estimated for the low-salinity pixels by adjusting pCO$_2$ for those pixels by the percentages given above and propagating these adjustments through air-sea flux calculations. We found for August 2004 that the sensitivity of air-sea flux estimates to underestimates in the <10 salinity range was negligible (<0.1%), while for April 2006, adjusting the low-salinity values resulted in fluxes shifting from a net uptake of carbon to net

Table 3. Air-Sea Flux Estimates for Specified Regions Based on Wind Speed Parameterizations and Satellite-Derived Estimates of pCO$_2$[a]

| Date | Region | Average Air-Sea CO$_2$ Flux (mmol m^{-2} d^{-1}) | | |
		Plume	Shelf	Entire Image
Aug 2004	W1992	−1.70	0.227	−1.17
	N2000	−1.72	0.230	−1.18
	H2006	−1.39	0.186	−0.96
Oct 2005	W1992	5.13	3.32	5.40
	N2000	4.39	2.84	4.63
	H2006	4.20	2.71	4.42
Apr 2006	W1992	−2.96	−1.18	1.24
	N2000	−2.76	−1.10	1.15
	H2006	−2.43	−0.97	1.01

[a]W1992, *Wanninkhof* [1992]; N2000, *Nightingale et al.* [2000]; H2006, *Ho et al.* [2006]. Positive values of CO$_2$ flux are in the direction of water to air.

release to the atmosphere for the plume region. In addition, adjusted CO$_2$ fluxes to the atmosphere were a factor of four higher for the entire image region. Clearly, these extrapolations are dependent on the validity of the assumption that the low-salinity conditions in the river were representative of other low-salinity pixels. These uncertainties highlight the need for more extensive in situ observations to better constrain the algorithms, particularly in low-salinity regions that may have a disproportionate impact on net fluxes.

[32] We similarly examined the sensitivity of air-sea flux estimates to observed differences between satellite-estimated and in situ observations of pCO$_2$ seen for the 24–26 salinity range in August 2004 and for the 10–20 salinity range in April 2006. Adjustment of the satellite-derived estimates of pCO$_2$ for the August 2004 24–26 salinity range data to agree with the in situ mean value resulted in an 18% greater net uptake of CO$_2$ in the plume region and a 14% greater net uptake for the overall image. There was no impact on shelf fluxes. Adjusting the April 2006 10–20 salinity range satellite estimates of pCO$_2$ to be consistent with in situ data for the same range resulted in greater negative CO$_2$ fluxes in the plume region and a decrease in sea-to-air CO$_2$ fluxes for the entire image area by a factor of 44%. The overall conclusion from these analyses was that observed offsets between satellite-derived and in situ pCO$_2$ values generally had a relatively small impact on regional air-sea flux estimates, with the exception of the April 2006 data and, particularly, in the case of the <10 salinity data for that period.

5. Summary and Conclusions

[33] To summarize, our estimates of air-sea fluxes for the plume region supported a net uptake for August 2004 and April 2006 (but with large uncertainties based on the sensitivity analyses), and a net source of CO$_2$ in October 2005 (Table 3). For shelf waters, air-sea exchange of CO$_2$ was near equilibrium in August 2004 and exhibited a net uptake of carbon in April 2006. For the entire image region, air-sea fluxes were negative in August 2004 and net positive in April 2006 and October 2005. The ranges of estimated air-to-sea fluxes were similar in magnitude to values reported by *Lohrenz and Cai* [2006] for June 2003.

[34] Air-sea fluxes during the October 2005 cruise were notably higher than during other cruises. The October 2005 cruise occurred during a period of low river discharge, which may have resulted in reduced primary production and autotrophic carbon fixation. Indeed, a higher range of chlorophyll values was observed during August 2004 and April 2006 as compared to October 2005 (data not shown), which would be consistent with lower rates of primary production during October 2005. In addition, as previously noted, the October 2005 cruise followed two major storm events (Katrina and Rita), which may have contributed to increased terrestrial inputs of organic matter and possibly enhanced remineralization due to sediment resuspension. An additional factor that likely contributed to the high pCO$_2$ in October 2005 was the breakdown of vertical stratification (i.e., water column structure was characterized by a weak vertical salinity gradients, data not shown). The intense mixing associated with the hurricanes dissipated hypoxic conditions in bottom waters [*Rabalais et al.*, 2007], presumably due to ventilation of bottom waters. Hypoxic

bottom waters have been observed to have high levels of DIC (and thus pCO$_2$ levels) (W. Cai, unpublished data, 2009), and vertical mixing of the high CO$_2$ deep water could explain the high surface pCO$_2$ observed in October 2005. While the events associated with hurricanes Katrina and Rita may represent extreme conditions, strong storms occur frequently, although episodically in space and time, in the Gulf of Mexico, and hypoxia is an annual phenomenon. Therefore, such high CO$_2$ release events cannot be ignored in annual flux estimates and require more study.

[35] It is reasonable to speculate that the air-sea flux of CO$_2$ would exhibit a seasonal pattern in this region driven by changes in the intensity of the biological pump. Such a seasonal cycle would be expected to be related to both river discharge and environmental forcing (nutrients, mixing and irradiance) [*Lohrenz et al.*, 2008b; *Lohrenz et al.*, 1999]. This seasonality is also in phase with hypoxia in bottom waters that occurs over large areas of the continental shelf off Louisiana and has been attributed to nutrient enhanced primary production [*Rabalais et al.*, 2002]. It follows that the quantification of air-sea fluxes of CO$_2$ may help in better understanding carbon dynamics related to other ecosystem processes such as supply of organic matter to bottom waters, which is a contributing factor to hypoxia. However, more observations are required to resolve the seasonal pattern in air-sea fluxes of CO$_2$ and their relationship to carbon dynamics in this system.

[36] Our findings raise questions about the magnitude of coastal air-sea fluxes of CO$_2$ in the northern Gulf of Mexico and point out the high degree of uncertainty in such estimates stemming from a lack of sufficient observations in this region. In a recent synthesis of coastal carbon fluxes based on a very limited set of offshore data in the northern Gulf, *Chavez et al.* [2007] reported average values for sea-to-air fluxes of CO$_2$ for coastal waters of the Gulf of Mexico of 9.4+24 g C m^{-2} y^{-1} (2.2+5.5 mmol C m^{-2} d^{-1}). While this assessment was not inconsistent with our observations during October 2005 and April 2006, our results during August 2004 and those published previously for June 2003 [*Lohrenz and Cai*, 2006] provide evidence that the region may at times be a net sink rather than source of CO$_2$. *Kortzinger* [2003] similarly reported low surface water CO$_2$ fugacity in the Amazon plume and attributed this in part to biological productivity in plume waters. Biological productivity likely contributed to a drawdown of CO$_2$ in Mississippi River plume-influenced surface waters as well [*Cai*, 2003].

[37] Other studies of air-sea flux of CO$_2$ for coastal waters encompass a range of values comparable to the range of values determined in this study. *Jiang et al.* [2008], using an extensive series of in situ observations of surface pCO$_2$ determined that the South Atlantic Bight was an overall net sink for CO$_2$ on an annual basis, and reported average rates of -1.4 − 1.2 mol C m^{-2} y^{-1} (−3.8 − 3.3 mmol C m^{-2} d^{-1}), which was within the range of values observed in this current study (Table 3). For west coast upwelling systems, both net uptake and release of CO$_2$ have been reported, including *Freiderich et al.* [2002] who reported average ocean-to-atmosphere fluxes of 1.5–2.2 mol C m^{-2} y^{-1} (4.1 − 6.0 mmol C m^{-2} d^{-1}) for a coastal upwelling system off central California, and *Hales et al.* [2005], who estimated a net ocean

uptake flux of −20 mmol C m^{-2} d^{-1} in a region of coastal upwelling off Oregon.

[38] Our results provide evidence that the Mississippi River outflow region of the northern Gulf of Mexico may act either as a source or a sink for atmospheric carbon dioxide depending on the seasonal and river discharge conditions. This result is consistent with recent syntheses that have examined the importance of coastal ecosystems in regional and global carbon budgets [*Borges et al.*, 2005; *Borges et al.*, 2006; *Cai et al.*, 2006]. These studies noted a latitudinal gradient with high and mid-latitude marginal seas acting as a sink and low latitude marginal seas as a source of atmospheric CO₂. From our very limited data set, the northern Gulf of Mexico appears to be a "transitional" system, acting at times as a source and other times as a sink for CO₂. The system state appears to be influenced by seasonal conditions as well as organic matter sources and net community production, factors noted by *Borges et al.* [2006] as important drivers for CO₂ dynamics in European coastal waters. The prior studies also point out the potentially high magnitude and variability of fluxes in coastal waters. Moreover, they note in particular the high uncertainties associated with the assessments of estuarine and plume regions. Our results underscore these points. For example, the satellite assessments revealed localized areas with both high and low surface water *p*CO₂ (Figure 6), and consequently high and low fluxes across the air-water interface. *Chen and Borges* [2009] noted that high carbon fluxes associated with inner estuaries may be a critical element in reconciling coastal carbon budgets and that inner estuaries may be sites of high rates of removal of terrestrial/riverine organic carbon. Our satellite extrapolations yielded results supporting the view that inshore waters were a source of CO₂. However, as was noted for the April 2006 data, uncertainties for the low salinity data require more extensive in situ validation to confirm these findings.

[39] Satellite observations can play an important role in refining estimation of coastal carbon cycling and extending the spatial and temporal coverage for assessments of *p*CO₂ distributions and air-sea fluxes of CO₂. Efforts to improve performance of algorithms for estimating air-sea flux of CO₂ and extend their applicability will require a better understanding of underlying processes driving variations in carbon system properties coupled with more sustained and extensive in situ data, including field-based surveys and time-series observations.

Notation

a_{CDOM} absorption due to chromophoric dissolved organic matter (m^{-1}).
a_p absorption due to particulate matter (m^{-1}).
a_{ph} absorption due to phytoplankton pigments (m^{-1}).
A_f absorptance of a filtered sample (unitless).
d_g geometric path length for filter pad absorption (m).
F_{chl} chlorophyll fluorescence as determined by the ship's underway fluorometer (arbitrary units).
F_{CO2} air-water flux of CO₂ (mmol m^{-2} d^{-1}).
k gas transfer velocity (piston velocity) of CO₂ (cm h^{-1}).
K_0 solubility coefficient of CO₂ at the in situ temperature and salinity (mol L^{-1} atm^{-1}).

pCO₂ partial pressure of CO₂ measured either in air or water (μatm).
T_b transmittance of a blank filter (unitless).
T_s transmittance of a filtered sample (unitless).
$β$ path length amplification factor for filter pad absorption.

References

Baith, K., R. Lindsay, G. Fu, and C. R. McClain (2001), SeaDAS, a data analysis system for ocean-color satellite sensors, *EOS Trans. AGU*, *82*, 202.

Borges, A. V. (2005), Do we have enough pieces of the jigsaw to integrate CO₂ fluxes in the coastal ocean?, *Estuaries*, *28*(1), 3–27.

Borges, A. V., B. Delille, and M. Frankignoulle (2005), Budgeting sinks and sources of CO₂ in the coastal ocean: Diversity of ecosystems counts, *Geophys. Res. Lett.*, *32*, L14601, doi:10.1029/2005GL023053.

Borges, A. V., L. S. Schiettecatte, G. Abril, B. Delille, and F. Gazeau (2006), Carbon dioxide in European coastal waters, *Estuarine Coastal Shelf Sci.*, *70*(3), 375–387.

Cai, W.-J. (2003), Riverine inorganic carbon flux and rate of biological uptake in the Mississippi River plume, *Geophys. Res. Lett.*, *30*(2), 1032, doi:10.1029/2002GL016312.

Cai, W.-J., and S. E. Lohrenz (2010), The Mississippi River plume and adjacent margin in the Gulf of Mexico, in *Carbon and Nutrient Fluxes in the Continental Margins: A Global Synthesis*, edited by K.-K. Liu et al., pp. 406–422, Springer, Berlin.

Cai, W.-J., M. H. Dai, and Y. C. Wang (2006), Air-sea exchange of carbon dioxide in ocean margins: A province-based synthesis, *Geophys. Res. Lett.*, *33*, L12603, doi:10.1029/2006GL026219.

Cai, W.-J., X. Guo, C.-T. A. Chen, M. Dai, L. Zhang, W. Zhai, S. E. Lohrenz, and Y. Wang (2008), A comparative overview of weathering intensity and HCO₃-flux of the world's major rivers with emphasis on the Changjiang, Huanghe, Pearl and Mississippi rivers, *Cont. Shelf Res.*, *28*(12), 1538–1549.

Chavez, F., T. Takahashi, W.-J. Cai, G. Friederich, B. Hales, R. Wanninkhof, and R. A. Feely (2007), Coastal oceans, in *The First State of the Carbon Cycle Report (SOCCR): The North American Carbon Budget and Implications for the Global Carbon Cycle. A Report by the U.S. Climate Change Science Program and the Subcommittee on Global Change Research*, edited by A. W. King et al., chap. 15, pp. 157–166, Natl. Climat. Data Cent., Natl. Oceanic and Atmos. Admin., Asheville, N. C.

Chen, C. T. A., and A. V. Borges (2009), Reconciling opposing views on carbon cycling in the coastal ocean: Continental shelves as sinks and near-shore ecosystems as sources of atmospheric CO₂, *Deep Sea Res. Part II*, *56*(8–10), 578–590.

Chen, C.-T. A., W. Zhai, and M. Dai (2008), Riverine input and air-sea CO₂ exchanges near the Changjiang (Yangtze River) Estuary: Status quo and implication on possible future changes in metabolic status, *Cont. Shelf Res.*, *28*(12), 1476–1482.

D'Sa, E. J., R. L. Miller, and C. Del Castillo (2006), Bio-optical properties and ocean color algorithms for coastal waters influenced by the Mississippi River during a cold front, *Appl. Opt.*, *45*(28), 7410–7428.

Dagg, M. J., and G. A. Breed (2003), Biological effects of Mississippi River nitrogen on the northern gulf of Mexico—A review and synthesis, *J. Mar. Syst.*, *43*(3–4), 133–152.

Dagg, M. J., R. Benner, S. Lohrenz, and D. Lawrence (2004), Transformation of dissolved and particulate materials on continental shelves influenced by large rivers: Plume processes, *Cont. Shelf Res.*, *24*(7–8), 833–858.

Del Castillo, C. E., and R. L. Miller (2008), On the use of ocean color remote sensing to measure the transport of dissolved organic carbon by the Mississippi River plume, *Remote Sens. Environ.*, *112*(3), 836–844.

DeMaster, D. J., W. O. Smith Jr., D. M. Nelson, and J. Y. Aller (1996), Biogeochemical processes in Amazon shelf waters: Chemical distributions and uptake rates of silicon, carbon and nitrogen, *Cont. Shelf Res.*, *16*, 617–643.

Feldman, G. C., and C. R. McClain (2007), Ocean Color Web: MODIS Aqua Reprocessing 5.1, http://oceancolor.gsfc.nasa.gov/REPROCESSING/Aqua/R1.1/, NASA Goddard Space Flight Cent., Greenbelt, Md.

Friederich, G. E., P. M. Walz, M. G. Burczynski, and F. P. Chavez (2002), Inorganic carbon in the central California upwelling system during the 1997–1999 El Nino–La Nina event, *Prog. Oceanogr.*, *54*(1–4), 185–203.

Goolsby, D. A., W. A. Battaglin, G. B. Lawrence, R. S. Artz, B. T. Aulenbach, R. P. Hooper, D. R. Keeney, and G. J. Stensland (1999), Flux and sources of nutrients in the Mississippi–Atchafalaya River basin: Topic 3 report for the integrated assessment on hypoxia in the Gulf of Mexico, *NOAA Decis. Anal. Ser. Rep. 17*, 130 pp., U.S. Dep. of Commer., Coastal Ocean Prog., NOAA, Silver Spring, Md.

Hales, B., T. Takahashi, and L. Bandstra (2005), Atmospheric CO_2 uptake by a coastal upwelling system, *Global Biogeochem. Cycles*, *19*, GB1009, doi:10.1029/2004GB002295.

Ho, D. T., C. S. Law, M. J. Smith, P. Schlosser, M. Harvey, and P. Hill (2006), Measurements of air-sea gas exchange at high wind speeds in the Southern Ocean: Implications for global parameterizations, *Geophys. Res. Lett.*, *33*, L16611, doi:10.1029/2006GL026817.

Jiang, L. Q., W. J. Cai, R. Wanninkhof, Y. C. Wang, and H. Luger (2008), Air-sea CO_2 fluxes on the US South Atlantic Bight: Spatial and seasonal variability, *J. Geophys. Res.*, *113*, C07019, doi:10.1029/2007JC004366.

Kortzinger, A. (2003), A significant CO_2 sink in the tropical Atlantic Ocean associated with the Amazon River plume, *Geophys. Res. Lett.*, *30*(24), 2287, doi:10.1029/2003GL018841.

Lefevre, N., J. Aiken, J. Rutllant, G. Daneri, S. Lavender, and T. Smyth (2002), Observations of pCO_2 in the coastal upwelling off Chile: Spatial and temporal extrapolation using satellite data, *J. Geophys. Res.*, *107*(C6), 3055, doi:10.1029/2000JC000395.

Lohrenz, S. E., and W.-J. Cai (2006), Satellite ocean color assessment of air-sea fluxes of CO_2 in a river-dominated coastal margin, *Geophys. Res. Lett.*, *33*, L01601, doi:10.1029/2005GL023942.

Lohrenz, S. E., M. J. Dagg, and T. E. Whitledge (1990), Enhanced primary production at the plume oceanic interface of the Mississippi River, *Cont. Shelf Res.*, *10*(7), 639–664.

Lohrenz, S. E., G. L. Fahnenstiel, D. G. Redalje, G. A. Lang, X. Chen, and M. J. Dagg (1997), Variations in primary production of northern Gulf of Mexico continental shelf waters linked to nutrient inputs from the Mississippi River, *Mar. Ecol. Prog. Ser.*, *155*, 45–54.

Lohrenz, S. E., G. L. Fahnenstiel, D. G. Redalje, G. A. Lang, M. J. Dagg, T. E. Whitledge, and Q. Dortch (1999), Nutrients, irradiance, and mixing as factors regulating primary production in coastal waters impacted by the Mississippi River plume, *Cont. Shelf Res.*, *19*(9), 1113–1141.

Lohrenz, S. E., A. D. Weidemann, and M. Tuel (2003), Phytoplankton spectral absorption as influenced by community size structure and pigment composition, *J. Plankton Res.*, *22*, 639–657.

Lohrenz, S. E., W. J. Cai, X. Chen, and M. Tuel (2008a), Satellite assessment of bio-optical properties of northern Gulf of Mexico coastal waters following hurricanes Katrina and Rita, *Sensors*, *8*, 4135–4150.

Lohrenz, S. E., D. G. Redalje, W.-J. Cai, J. Acker, and M. Dagg (2008b), A retrospective analysis of nutrients and phytoplankton productivity in the Mississippi River plume, *Cont. Shelf Res.*, *28*(12), 1466–1475.

Maritorena, S., D. A. Siegel, and A. R. Peterson (2002), Optimization of a semianalytical ocean color model for global-scale applications, *App. Opt.*, *41*(15), 2705–2714.

Milliman, J. D., and R. H. Meade (1983), World-wide delivery of river sediment to the oceans, *J. Geol.*, *91*, 1–21.

Murata, A. (2006), Increased surface seawater pCO_2 in the eastern Bering Sea shelf: An effect of blooms of coccolithophorid Emiliania huxleyi?, *Global Biogeochem. Cycles*, *20*, GB4006, doi:10.1029/2005GB002615.

Nightingale, P. D., G. Malin, C. S. Law, A. J. Watson, P. S. Liss, M. I. Lidicoat, J. Boutin, and R. C. Upstill-Goddard (2000), In situ evaluation of air-sea gas exchange parameterizations using novel conservative and volatile tracers, *Global Biogeochem. Cycles*, *14*(1), 373–387, doi:10.1029/1999GB900091.

Olsen, A., J. A. Trinanes, and R. Wanninkhof (2004), Sea-air flux of CO_2 in the Caribbean Sea estimated using in situ and remote sensing data, *Remote Sens. Environ.*, *89*(3), 309–325.

Ono, T., T. Saino, N. Kurita, and K. Sasaki (2004), Basin-scale extrapolation of shipboard pCO_2 data by using satellite SST and Chla, *Int. J. Remote Sens.*, *25*(19), 3803–3815.

Rabalais, N. N., R. E. Turner, and W. J. Wiseman (2002), Gulf of Mexico hypoxia, *Annu. Rev. Ecol. Syst.*, *33*, 235–263.

Rabalais, N. N., R. E. Turner, B. K. Sen Gupta, D. F. Boesch, P. Chapman, and M. C. Murrell (2007), Hypoxia in the northern Gulf of Mexico: Does the science support the plan to reduce, mitigate, and control hypoxia?, *Estuaries Coasts*, *30*(5), 753–772.

Riley, G. A. (1937), The significance of the Mississippi River drainage for biological conditions in the northern Gulf of Mexico, *J. Mar. Sci.*, *1*, 60–74.

Robbins, L. L., P. G. Coble, T. D. Clayton, and W.-J. Cai (2009), Ocean carbon and biogeochemistry scoping workshop on terrestrial and coastal carbon fluxes in the Gulf of Mexico, St. Petersburg, FL, May 6–8, 2008, *U.S. Geol. Surv. Open File Rep.*, *2009-1070*, 1–46. (Available at http://pubs.usgs.gov/of/2009/1070/.)

Tans, P. P. (2009), Trends in Carbon Dioxide, http://www.esrl.noaa.gov/gmd/ccgg/trends/, *NOAA Earth Syst. Res. Lab.*, Boulder, Colo.

Ternon, J., C. Oudot, A. Dessier, and D. Diverres (2000), A seasonal tropical sink for atmospheric CO_2 in the Atlantic ocean: The role of the Amazon River discharge, *Mar. Chem.*, *68*(3), 183–201.

Tsunogai, S., S. Watanabe, and T. Sato (1999), Is there a "continental shelf pump" for the absorption of atmospheric CO_2?, *Tellus Ser. B*, *51*(3), 701–712.

Wang, S. L., C. T. A. Chen, G. H. Hong, and C. S. Chung (2000), Carbon dioxide and related parameters in the East China Sea, *Cont. Shelf Res.*, *20*(4–5), 525–544.

Wang, Z. H. A., and W.-J. Cai (2004), Carbon dioxide degassing and inorganic carbon export from a marsh-dominated estuary (the Duplin River): A marsh CO_2 pump, *Limnol. Oceanogr.*, *49*(2), 341–354.

Wanninkhof, R. (1992), Relationship between wind speed and gas exchange over the ocean, *J. Geophys. Res.*, *97*(C5), 7373–7382, doi:10.1029/92JC00188.

Wright, V. (2005), Seasonal dynamics of colored dissolved organic matter in the Mississippi River plume and the Northern Gulf of Mexico, M.S. thesis, 68 pp., Univ. of South. Miss., Hattiesburg, Miss.

W.-J. Cai and F. Chen, Department of Marine Sciences, University of Georgia, Athens, GA 30602, USA. (wcai@uga.edu)

X. Chen, S. E. Lohrenz, and M. Tuel, Department of Marine Science, University of Southern Mississippi, 1020 Balch Blvd., Stennis Space Center, MS 39529, USA. (steven.lohrenz@usm.edu)